SALT-INDUCED AGGREGATION AND FUSION OF DIOCTADECYLDIMETHYLAMMONIUM CHLORIDE AND SODIUM DIHEXADECYLPHOSPHATE VESICLES

A. M. CARMONA-RIBEIRO AND H. CHAIMOVICH
Departamento Bioquímica, Instituto de Química, Universidade de São Paulo, CEP 20780, Brazil

ABSTRACT Small dioctadecyldimethylammonium chloride (DODAC) vesicles prepared by sonication fuse upon addition of NaCl as detected by several methods (electron microscopy, trapped volume determinations, temperature-dependent phase transition curves, and osmometer behavior. In contrast, small sodium dihexadecyl phosphate (DHP) vesicles mainly aggregate upon NaCl addition as shown by electron microscopy and the lack of osmometer behavior. Scatter-derived absorbance changes of small and large DODAC or DHP vesicles as a function of time after salt addition were obtained for a range of NaCl or amphiphile concentration. These changes were interpreted in accordance with a phenomenological model based upon fundamental light-scattering laws and simple geometrical considerations. Short-range hydration repulsion between DODAC (or DHP) vesicles is possibly the main energy barrier for the fusion process.

INTRODUCTION

Our understanding of structure and function of biological membranes has been greatly developed by using structures of defined chemical composition having just some of the properties of biological membranes (1). Another aspect that has emerged from membrane mimicking is a novel chemistry of both practical and theoretical utility (2, 3).

The general problem of stability of interacting membranes is relevant in many systems. The process of mutual approach of membranes leading to adhesion or fusion may be conveniently divided into three main stages: (*a*) mutual approach; (*b*) destabilization of the liquid film between the membranes and/or the membranes themselves; and (*c*) expansion of the area of membrane contact during adhesion or expansion of the hole during fusion (4). Phospholipid vesicles have been extensively used as models for membrane fusion studies. Interaction forces involved in the mutual approach of membranes have been used to describe salt-induced interaction of phospholipid (5–10) or surfactant (11) vesicles. Didodecyldimethylammonium bromide (DDAB) large vesicles fuse in the presence of micromolar concentrations of certain organic and inorganic divalent anions (12). We have suggested that small sonicated vesicles of dioctadecyldimethylammonium chloride (DODAC) and sodium dihexadecylphosphate (DHP) vesicles fuse upon addition of NaCl (11). Here we unequivocally demonstrate NaCl-induced fusion of small sonicated DODAC vesicles and present a model that describes vesicle aggregation and fusion. We also introduce a simple method for kinetic or equilibrium detection of the fusion of small vesicles.

Correspondence should be addressed to A. M. Carmona-Ribeiro.

MATERIAL AND METHODS

Dioctadecyldimethylammonium chloride (DODAC) and sodium dihexadecylphosphate (DHP) were purified and analyzed as described (11). Sephadex G-25 (fine) was obtained from Sigma Chemical Co. (St. Louis, MO) and (^{14}C)-sucrose from Schwarz-Mann (Orangeburg, NY) specific activity 480 mCi/mmol). All other reagents were analytical grade. Deionized water, doubly distilled in glass, was used throughout. DODAC and NaCl concentrations were determined by chloride microtitration (13) and DHP concentration by measuring phosphate (14).

Small DODAC or DHP vesicles were obtained by sonication (15, 16) and large DODAC or DHP vesicles by vaporization of a DODAC or DHP chloroformic solution in aqueous solutions (17, 18). Salt-induced turbidity changes of vesicle dispersions were followed by measuring absorbance at 400 nm in a Beckman M-25 Spectrophotometer. The time-lag between mixing and register start was usually <6 s. The scatter-derived absorbance will be referred to as absorbance hereafter. The osmolality of the aqueous solutions used to prepare the large vesicles and that of the salt solution added to the vesicles were kept equal. Osmotic gradients induce turbidity changes as a consequence of swelling or shrinking of the vesicles (17, 18). Osmolality values were adjusted in all cases with D-glucose and measured in an osmometer (model 2007; Precision Systems, Inc., Natick, MA).

For electron microscopy, aliquots of sonicated DODAC or DHP vesicles (2.5 mM) in the presence of NaCl (0.042 M) were mixed with an equal volume of ammonium molybdate (2%) or uranyl acetate (1%) for 30 s. After draining and drying, the sample was examined in a Zeiss EM-9 52 Electron Microscope (Carl Zeiss, Inc., Thornwood, NY) operated at 60 KV. From electron micrographs, histograms were obtained and mean external diameters calculated.

Changes of absorbance as a function of temperature were obtained in a Cary-14 Spectrophotometer (Applied Physics Corp., Monrovia, CA) equipped with a thermostatically controlled cell compartment coupled to a Haake F-12 Circulating Bath (Haake Buchler Instruments, Inc., Saddle Brook, NJ). Heating or cooling rates were usually 2°K/min.

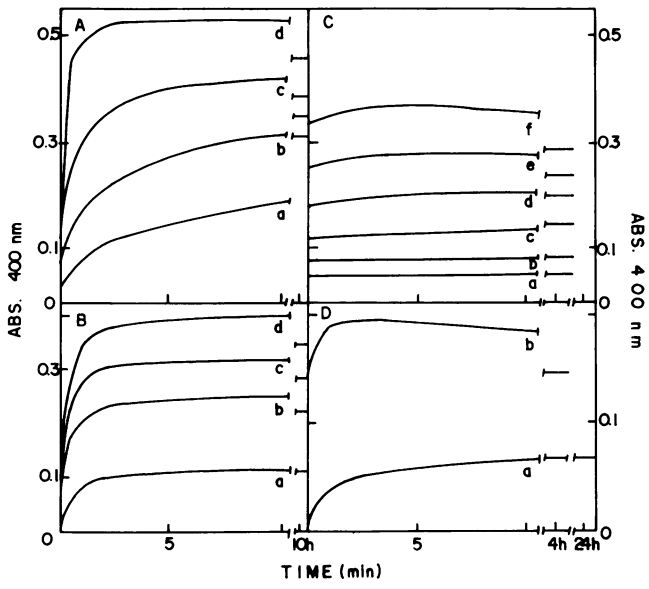

FIGURE 1 Scatter-derived absorbance change induced by NaCl on small (*A*, *B*, *D*) and large (*C*, *D*) DODAC vesicles. In *A*, DODAC concentration is 1.8 mM and NaCl concentration (mM) is 42 (*a*); 64 (*b*); 85 (*c*); 132 (*d*). In *B*, NaCl concentration is 0.117 M and DODAC concentration (mM) is 0.47 (*a*); 0.85 (*b*); 1.03 (*c*); 1.13 (*d*). In *C*, DODAC concentration is 0.26 mM and NaCl concentration (mM) is: 0 (*a*); 30 (*b*); 64 (*c*); 100 (*d*); 130 (*e*); 171 (*f*). In *D*, absorbance changes for small (*a*) and large (*b*) DODAC vesicles (0.35 mM) are compared in 110 mM NaCl. Large DODAC vesicles were prepared in 0.428 M D-glucose.

Temperatures were measured inside the cuvette with a copper-constantan thermocouple connected to a millivoltmeter. The response of this measuring system is linear between 0 and 100°C with a relative error of <0.01%.

Determination of internal volume (V) for sonicated DODAC vesicles upon salt addition was performed using (^{14}C)-sucrose as a marker (19). A typical experiment was as follows. Sonicated DODAC vesicles (10 mM) were prepared in 0.02 M sucrose. 5.0 ml of this preparation was mixed with 5 ml of a 0.02 M sucrose and 0.100 M NaCl solution containing (^{14}C)-sucrose. The time immediately after mixing was taken as zero time. Aliquots (0.02 ml) were then filtered through a Sephadex G-25 column (28 × 1 cm) previously saturated with sonicated DODAC vesicles and equilibrated with a 0.05 M NaCl and 0.02 M sucrose solution. Radioactivity and DODAC recoveries were higher than 93% in all cases. Radioactivity of the elution profiles was used for the calculation of V as described (17).

For determination of osmotic properties, vesicles in the presence of salt were added to aqueous solutions of NaCl (or NaCl plus erythritol) and the time-dependent absorbance changes were registered at 400 nm.

The initial shrinking rate (v_o%) was defined as: $v_o\% = (100/A_o) \cdot (\Delta A/\Delta t)$, where $\Delta A/\Delta t$ is the initial slope of the curve of absorbance vs. time and A_o, the initial absorbance. The reciprocal of the total absorbance change was normalized by using the parameter $A_o/\Delta A = A_o/(A_f - A_o)$ where A_o is the measured absorbance 24 h after the addition of vesicles to hypo- or hyperosmotic solutions. Mean values for these parameters were obtained from at least two independent experiments and errors are expressed as mean-square deviations.

RESULTS

To demonstrate the fusogenic effect of salt solutions on small sonicated DODAC vesicles, we characterized some physical and functional properties of the dispersions obtained upon NaCl addition. These properties were compared with those of the nontreated preparation and those of large DODAC vesicles obtained by chloroform vaporization (17).

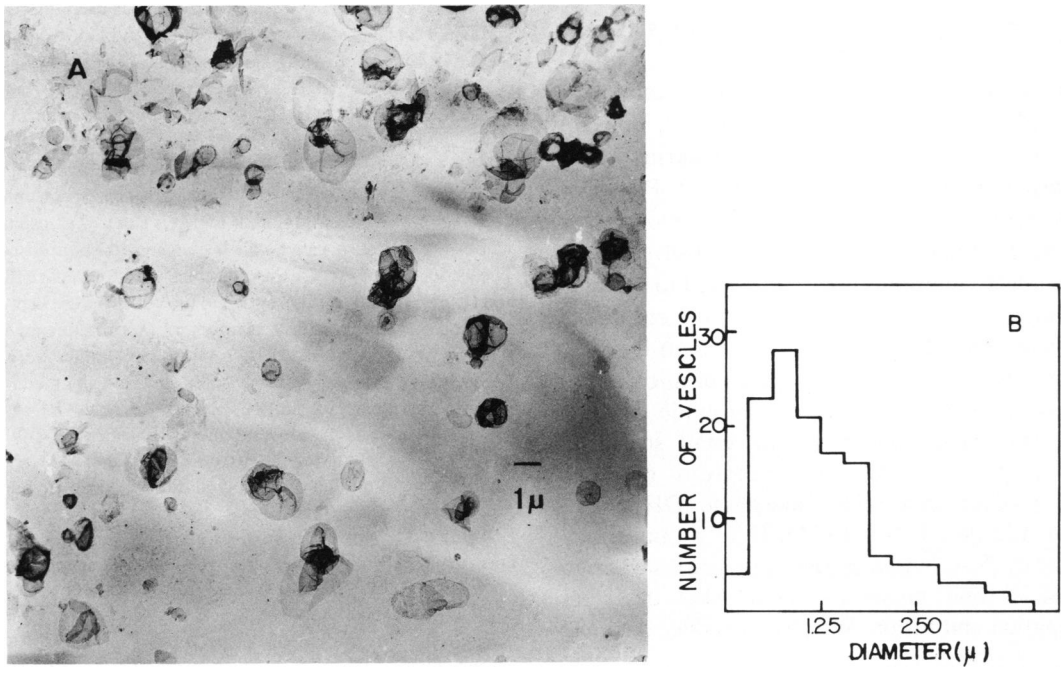

FIGURE 2 Electron microscopy of a positively stained preparation of sonicated DODAC vesicles (2.5 mM) 48 h after NaCl addition (0.042 M) (*A*). The distribution of vesicles size is displayed in *B*.

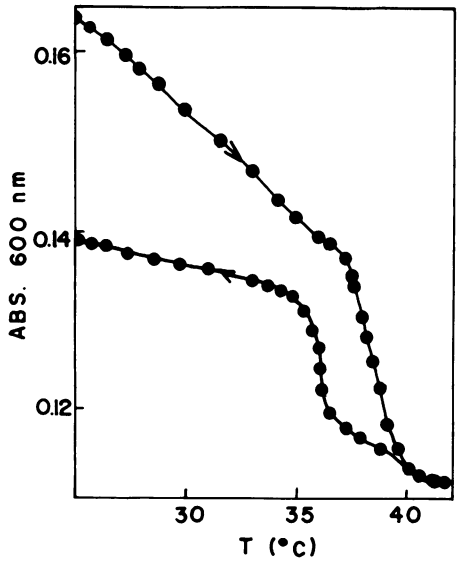

FIGURE 3 Temperature-induced phase transition of sonicated DODAC vesicles (2.5 mM) 7 h after NaCl addition (0.042 M). Cooling or heating is indicated by *arrows*.

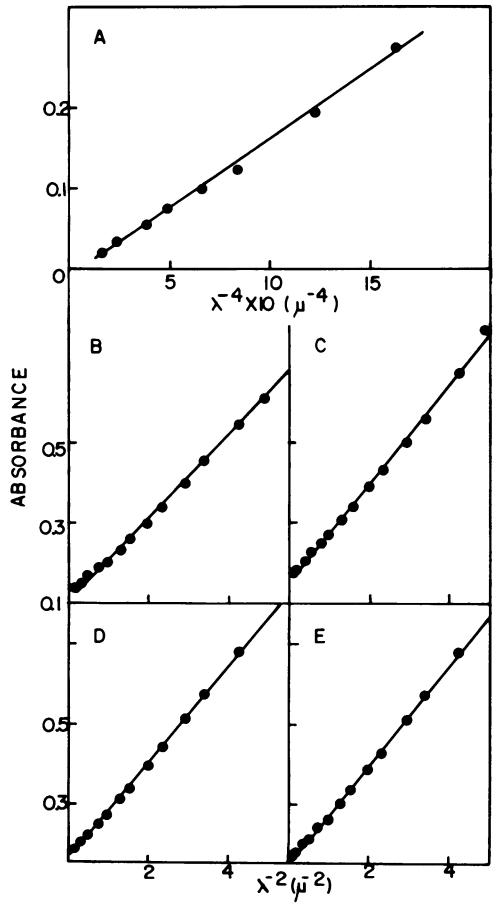

FIGURE 4 Spectra of sonicated DODAC vesicles (5 mM) prepared in water before (*A*) and 40 min (*B*), 3 h (*C*), 6 h (*D*), or 24 h (*E*) after NaCl addition (0.042 M). Final DODAC concentration in the sample containing salt is 2.5 mM.

Time-dependent absorbance changes obtained after salt addition for a range of salt (Fig. 1 *A*) or DODAC concentration (Fig. 1 *B*) were similar in shape to those obtained for large vesicles (Fig. 1 *C*). The change in absorbance as a function of time had three phases. There was an increase followed by a plateau then a decrease. For sonicated vesicles, this time-sequence was slower when compared with large DODAC vesicles (Fig. 1 *D*). DODAC dispersions remained homogeneous for at least 72 h after salt addition and began to become gelatinous after one month with no visible flocculation or precipitation.

Preparations of DODAC sonicated vesicles were examined by electron microscopy with both negative and positive staining 48 h after NaCl addition. The micrographs showed closed vesicular structures (Fig. 2 *A*) with a mean external diameter of 1.3 μm (range 0.2–4.0 μm, Fig. 2 *B*). This preparation will be hereafter referred to as fused DODAC vesicles.

The change of absorbance as a function of temperature for sonicated DODAC vesicles incubated for 7 h with a NaCl solution is shown in Fig. 3. The absorbance decreases monotonically with temperature. A sharp change in slope was observed around the (heating) transition temperature (38.6°C) and a pronounced hysteresis upon cooling (Fig. 3). A reproducible difference was detected between the absorbances observed before and after the heating-cooling cycle. The final absorbance after the temperature cycle remained unaltered (room temperature) for at least 24 h.

Absorbance (*A*) of sonicated DODAC vesicles prepared in water varied linearly with λ^{-4} (Fig. 4 *A*). This wavelength dependence remained unchanged for at least 24 h after preparation of the vesicles (13). After salt addition, *A* varied linearly with λ^{-2} (Fig. 4 *B–E*).

If a water-soluble impermeable marker such as (^{14}C)-sucrose (17) is added to sonicated DODAC vesicles, fusion can lead to an entrapment of the marker. This entrapment (*V*) can be used as a measure of fusion with time (19–21). For sonicated DODAC vesicles, *V* values increased as a function of time after salt addition (Fig. 5 *A*). This figure includes the *V* value calculated from electron micrographs (Fig. 2), taking 40 Å^2 as the mean area per DODAC monomer (22). For comparison, we also followed the corresponding absorbance changes after salt addition (Fig. 5 *B*, full circles) and plotted the slope of the curves depicted in Fig. 4 *B–E* as a function of time (Fig. 5 *B*, open circles). Curves on Fig. 5 *B* are similar in shape. In comparison with the curve of *V* as a function of time (Fig. 5 *A*), the attainment of the plateau is faster for curves on Fig. 5 *B*.

Osmotic gradients induced time-dependent absorbance changes in fused DODAC vesicles. When intravesicular NaCl concentration was higher than the external concentration, absorbance decreased with time (Fig. 6 *A–F*). When the concentration of impermeable solutes was higher in the external solution absorbance increased with time (Fig. 6 *G–P*).

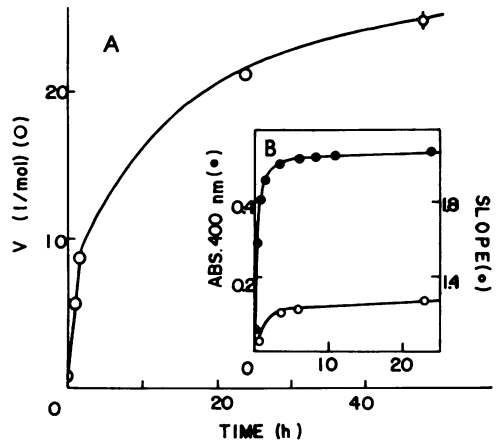

FIGURE 5 Internal volume (V) of sonicated DODAC vesicles (2.5 mM) prepared in 20 mM sucrose as a function of time after NaCl addition (0.042 M) (○) (A). (^{14}C)-sucrose was added to the sonicated vesicles prior to salt addition. At zero time, salt was added to the sonicated vesicles. Gel chromatography separated entrapped and free (^{14}C)-sucrose for calculation of V values. For comparison, the V value obtained from electron microscopy assuming 40 Å^2 as the area per monomer is also shown (◇) (A). Time-dependent absorbance changes of the same preparation of sonicated DODAC vesicles after salt addition (0.042 M) (•) and slopes against time for "spectra" from Fig. 4 (○) are in B.

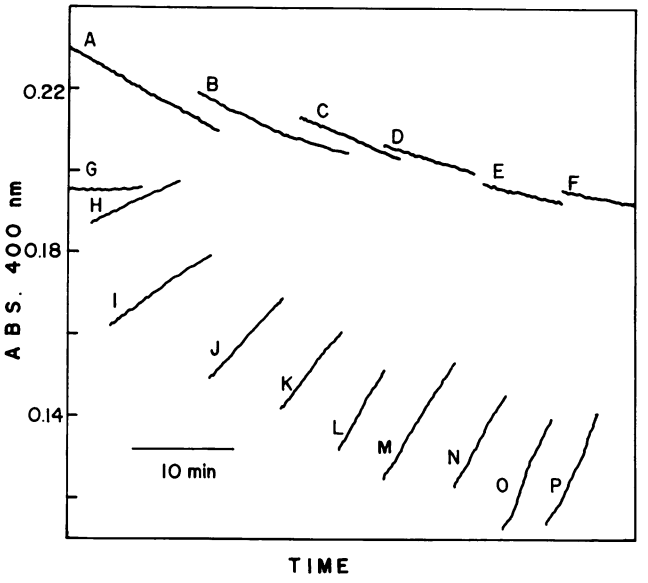

FIGURE 6 Time-dependent absorbance changes due to osmotic gradients imposed to DODAC vesicles at least 24 h after salt addition (0.057 M). Sonicated DODAC vesicles (10 mM) were prepared in water, NaCl was added to a final concentration of 0.057 M and, after 2 h, aliquots of this mixture (0.2 ml) were added to 0.8 ml water (A) or NaCl solution with the following concentration (in mM): 8 (A); 16 (B); 27 (C); 37 (D); 46 (E); 53 (F); 60 (G). For shrinking, 0.2 ml of the mixture containing the vesicles were added to 0.8 ml aqueous solutions containing 57 mM NaCl and erythritol in the following concentrations (in mM): 20 (H); 40 (i); 50 (j); 60 (K); 70 (L); 80 (M); 90 (N); 100 (O); 120 (P).

The initial shrinking rate (v_0 %) varied linearly with NaCl concentration gradient (ΔC NaCl) displaying two different slopes depending on the sign of the concentration gradient (Fig. 7 A). This difference could be associated with an increased permeability of the DODAC vesicle under hypotonic condition. The actual osmotic gradient would be smaller than that at time zero due to partial leakage of the contents of the vesicles as in the case of phospholipid liposomes (23). A linear relationship between v_0 % and ΔO (ER. + NaCl) was obtained for the absorbance changes induced by NaCl and erythritol (Fig. 7 C). $A_0/\Delta A$ varied linearly with the reciprocal of the NaCl concentration gradient (Fig. 7 B) or the NaCl plus erythritol osmolarity gradient (Fig. 7 D).

For sonicated DHP vesicles, time-dependent absorbance changes after salt addition for a range of salt (Fig. 8 A) or DHP concentration (Fig. 8 B) are similar to those for large DHP vesicles (Fig. 8 C). In these curves, the absorbance always increases as a function of time and no plateau is attained. Visual observations after 24 or 48 h showed particles in suspension that later precipitated.

DHP dispersions obtained after NaCl addition to sonicated vesicles, when examined by electron microscopy, showed small sonicated vesicles, aggregates of small sonicated vesicles and some large vesicles (Fig. 9). To confirm that the DHP vesicle population 24 h after salt addition was composed mainly of aggregates of small vesicles, we tested the dispersion behavior toward osmotic gradients. During the first 10 min following the osmotic shock no significant absorbance change could be detected. 24 h thereafter the absorbance was much higher than that expected if only shrinkage or swelling had occurred.

DISCUSSION

DODAC and DHP vesicles are suitable models for interfacial effects on chemical reactions (3), for permeability and transport studies (17, 18) and for membrane interactions induced by salts (11). In this section we show that the study of DODAC or DHP vesicles contributes to a better understanding of the relationship between monomer-structure and intervesicular interactions leading to membrane fusion.

It has been often pointed out that light scattering or turbidity measurements are unable to distinguish between vesicle aggregation and fusion (24–26). An analysis of the relative contributions of these processes using fundamental light-scattering theory in the context of a simple model for aggregation and fusion is lacking. Light scattering can follow the sample transformation without perturbation, an advantage which is absent for methods relying on the analysis of aliquots (electron microscopy, trapped volume, ultracentrifugation or gel chromatography) (26). Here we will try to overcome interpretative difficulties of turbidity data and propose a phenomenological model that is able to account for the scatter-derived absorbance changes observed for sonicated and large DODAC or DHP vesicles after NaCl addition (Fig. 1 and Fig. 8).

For spherical particles with a diameter D very small compared with the wavelength of light ($D \ll \lambda$), the

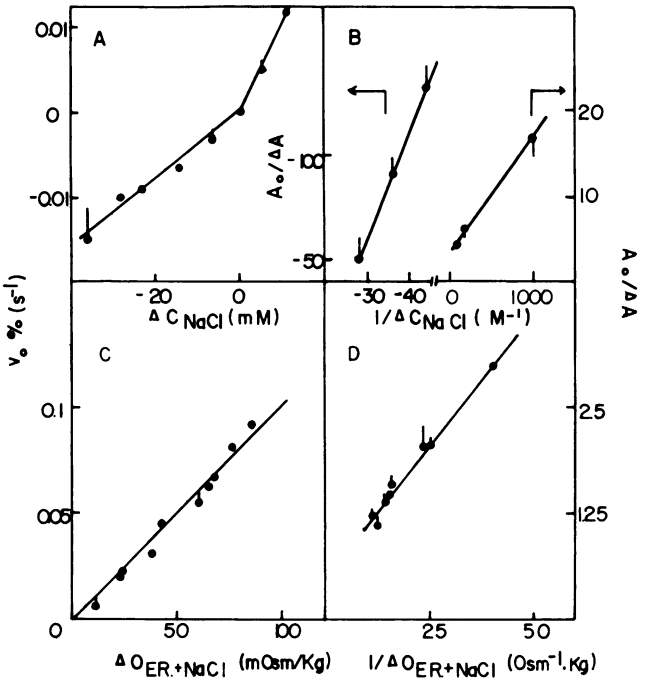

FIGURE 7 Osmometer behavior of a preparation containing sonicated DODAC vesicles in the presence of salt. Osmotic gradients were generated by NaCl or by NaCl plus erythritol and time-dependent absorbance changes as those in Fig. 6 were recorded permitting calculations of osmometer parameters. Initial swelling or shrinking rates (v_0 %) were plotted against the NaCl concentration gradient (ΔC NaCl) (A) or against the NaCl plus erythritol osmolarity gradient (ΔO NaCl + ER) (C). The extension of swelling or shrinkage ($A_0/\Delta A$) was plotted against the reciprocal of the concentration gradient of NaCl ($1/\Delta C$ NaCl) (B) or against the reciprocal of the osmolarity gradient of NaCl plus erythritol ($1/\Delta O$ NaCl + ER) (D).

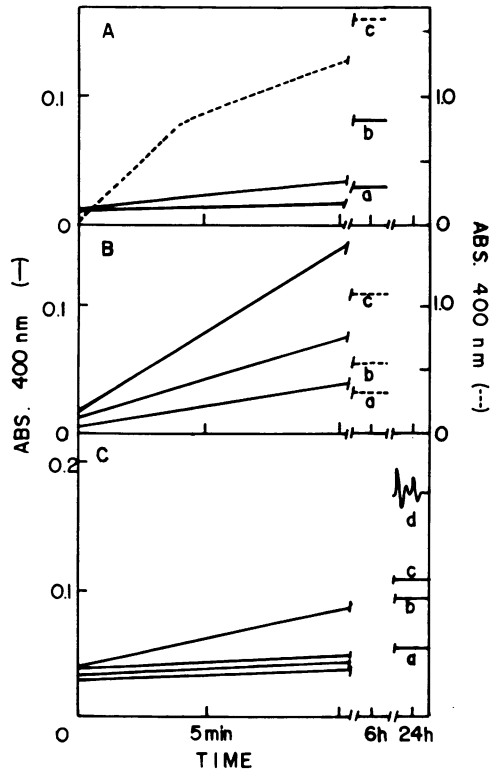

FIGURE 8 Scatter-derived absorbance changes induced by NaCl on small (A, B) and large (C) DHP vesicles. In A, DHP concentration is 0.57 mM and salt concentration (in mM) is 53.7 (a), 85.0 (b), and 132.2 (c). In B, NaCl concentration is 110 mM and DHP concentration (mM) is 0.23 (a); 0.34 (b), and 0.57 (C). In C, large DHP vesicles (0.62 mM) prepared in 0.430 M D-glucose are in NaCl concentrations (mM) of: 70 (a); 127 (b); 153 (c); and 171 (d).

scatter-derived absorbance (A) is given by (27)

$$A = [32\pi^3/(2.3 \cdot 3 \cdot n_0^2)] \cdot (dn/dc)^2 \cdot q^2 \nu \lambda^{-4} \quad (1)$$

where dn/dc is the specific refractive index increment, n_0 the refractive index of the medium, q the anhydrous mass of the scattering particle, ν the number of particles per unit volume, and λ the wavelength of the incident radiation. Assuming that dn/dc does not change upon aggregation, the ratio between the absorbance before (A_0) and after (A_t) aggregation is simply

$$A_t/A_0 = i, \quad (2)$$

where i is the number of vesicles in the aggregate. Upon aggregation, the absorbance will increase as long as the effective size of the aggregate remains lower than λ.

If the particles are not small with respect to λ, phase changes of the light will occur within the particle and the scattered light will interfere (28). For particles of dimensions comparable to λ ($D \approx \lambda$) and index of refraction similar to that of the medium, the Jobst law can be applied (29)

$$A = (5.984/n_0^2)\,(dn/dc)^2\, q^2\, \nu\, R^{-2}\, \lambda^{-2}, \quad (3)$$

where R is the particle radius.

In this range of particle size the absorbance is linearly dependent on λ^{-2} (Eq. 3 and Fig. 4 *B–D*). Under these conditions, an increase in the slope of the function relating A with λ^{-2} implies that the anhydrous mass increase is larger than that of the particle size (R). The A_t/A_0 value will depend exclusively upon the ratio between the number of aggregated particles (i) and the square of the ratio between the radius of the original particle (r) and that of the aggregate (R')

$$A_t/A_0 = i\,(r/R')^2. \quad (4)$$

From Eq. 4, a decrease in absorbance ($A_t < A_0$) is due to aggregation of large vesicles ($i < 4$). This interpretation is unambiguous since fusion of large vesicles in an aggregate with radius r (giving a fused vesicle with radius R') will necessarily imply $R' < r$ and $A_t > A_0$. Both statements can be easily verified using Eq. 4 and geometrical calculations of r and R' for symmetrical aggregated or fused forms.

On the other hand, if $D \ll \lambda$, Eq. 1 must be applied and the independence of A on the particle size implies that fusion of vesicles composing an aggregate cannot be detected and an absorbance increase necessarily results from aggregation of small vesicles.

Using the condition of validity of the Jobst approxima-

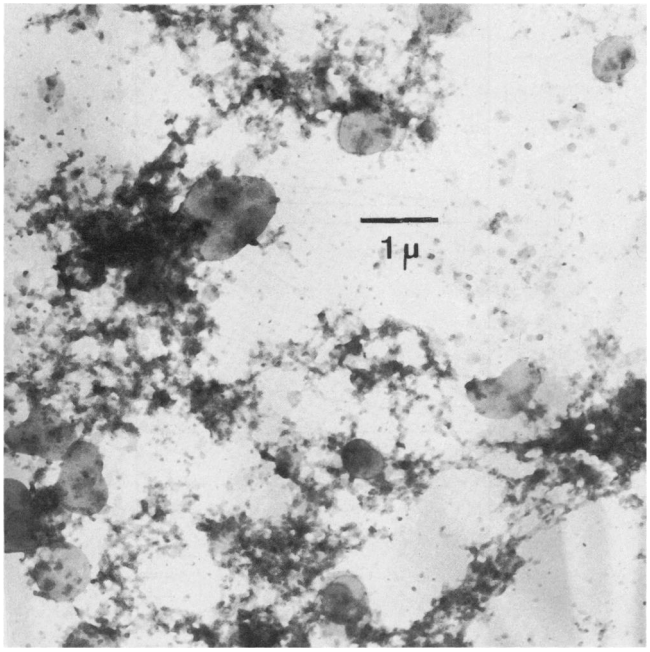

FIGURE 9 Electron microscopy of a positively stained preparation of sonicated DHP vesicles (2.5 mM) 48 h after NaCl addition (0.042 M).

tion ($D \approx \lambda$), the particle diameter must be within 4,000 to 8,000 Å (visible range). Fused vesicles possessing diameters in the range of 4,000 to 8,000 Å may be thought as the fusion product of n vesicles with radius r (in Å), where n varies between $(2{,}000/r)$ and $(4{,}000/r)$. Therefore, the attainment of the absorbance decrease phase (Fig. 1) due to aggregation of large vesicles depends on the mutual approach, adhesion and fusion of 169–679 small vesicles (r = 150 Å) or 4–16 large vesicles (r = 2,000 Å). This analysis makes reasonable the retarded absorbance decrease phase for sonicated DODAC vesicles after salt addition as compared with the rapid attainment of the same phase for the large DODAC vesicles (Fig. 1 *D*).

The possibilities of the model may be further explored by supposing small vesicles (~150 Å mean diameter) which only aggregate. An absorbance increase due to small vesicle aggregation will be observed (Eq. 2). As the aggregate size increases and the dimension of the aggregate compares with λ, further aggregation of small vesicles yielding a large aggregate would also result in an absorbance increase (from Eq. 4 and simple geometrical calculations of R' by supposing for example, the formation of cubic aggregates with 27, 64, 125 small vesicles with radius r). Thus, the absorbance, for a small vesicle system which undergoes only aggregation, increases progressively with time. Aggregates can grow until the formation of flocs in suspension yields first an oscillation in absorbance (Fig. 8 *C*, curve *d*) and finally precipitation as was shown for DHP vesicles after salt addition (Fig. 8 *A–C*).

Eqs. 1 and 3 can also be analyzed with respect to osmotic effects in vesicular systems. Swelling or shrinkage of small vesicles ($D \ll \lambda$) due to osmotic gradients do not alter the absorbance (17, 30), as predicted from Eq. 1. On the other hand, particle size variations due to osmotic effects on large vesicles ($D \approx \lambda$) produce an absorbance increase due to shrinkage and an absorbance decrease due to swelling (31, 32). Small aggregated vesicles should not exhibit absorbance variations due to osmotic gradients but large fused vesicles should. On this basis, we propose a method for detection of fusion and discrimination between aggregation of small vesicles and fusion based on the determination of osmometer behavior. Sonicated DODAC vesicles, 24 h after salt addition, behaved as an osmometer towards osmotic gradients of NaCl or NaCl and erythritol (Fig. 6 and 7), a fact which strongly suggests the presence of large fused vesicles in significant proportions. The lack of osmotic response in sonicated DHP vesicles 24 h after salt addition shows that large fused vesicles are not present in significant proportions. Both conclusions were confirmed by the electron micrographs (Figs. 2 and 9). DHP sonicated vesicles fuse to some extent (11) after salt addition as shown by the decay of the excimer-monomer ratio of a lipid fluorescent probe (19). However, both the shape of the time-dependent absorbance changes after salt addition (Fig. 8) and the absence of osmometer behavior suggest that fusion is not frequent.

Below the phase transition temperature (T_c), the occurrence of aggregation only or of aggregation followed by fusion will depend on the vesicle concentration range. For dipalmitoylphosphatidylcholine (DPPC) (4°C) in the 0.5–5.0 mM (Pi) concentration range, small vesicles aggregate and the size of the aggregates increases linearly with time (33). In the 20–120 mM Pi range, small DPPC vesicle aggregation is followed by fusion (33). Analogously, fusion of sonicated DHP vesicles will possibly be more frequent at DHP concentrations higher than those used in this study. Furthermore, for DPPC vesicles (4°C and 0.5–5.0 mM Pi) aggregation increases with time until the aggregates precipitate (28), in close analogy with the behavior of our sonicated DHP vesicles after salt addition.

Eqs. 1 to 4, associated with simple geometrical calculation, lead to interpretations summarized in Table I.

Particles formed upon NaCl addition to sonicated DODAC vesicles are shown, by a variety of methods (Figs. 3 to 7 and reference 11), to be large vesicles. For this to be the case, it is necessary for aggregation to be faster than fusion. That this is in fact the case can be seen by comparing the time-course of the scatter-derived absorbance increase and of the slope increase (Fig. 5 *B*), which reflect both fusion and aggregation, with the time-course of fusion alone, as assessed by the internal volume (V) increase (Fig. 5 *A*). For example, 2 h after salt addition, V is ~9 l/mol, i.e., only ~40% of the value attained after 24 h, whereas the absorbance value is 0.47, i.e., 87% of the value at 24 h. Therefore, at 2 h, the small sonicated vesicles were aggregated, in addition to being ~40% fused.

Sonicated DODAC vesicles exhibit a relatively broad phase transition temperature range when compared with

TABLE I
PHENOMENA ASSOCIATED WITH TIME-DEPENDENT ABSORBANCE CHANGES FOR INTERACTING VESICLES IN ACCORDANCE WITH THE SCATTERING LAWS

Absorbance behavior	Vesicle diameter (D)	
	$D << \lambda$	$D \approx \lambda$
Increase	1. Aggregation of small vesicles.	1. Fusion of large vesicles composing a large aggregate.
	2. Small aggregates further aggregating small vesicles.	2. Fusion of small vesicles composing a large aggregate.
	3. Disaggregation of large vesicles from large vesicle aggregates.	3. Shrinkage of large vesicles.
Decrease	1. Disaggregation of small vesicles.	1. Aggregation of large vesicles ($i < 4$).
	2. Vesicles yielding micelles.	2. Swelling of large vesicles.
Invariancy	1. Fusion of small vesicles composing a small aggregate.	
	2. Shrinkage or swelling of small vesicles.	

large DODAC vesicles (17). Seven hours after salt addition both the phase transition temperature range and the T_c values of salt-treated sonicated DODAC vesicles (Fig. 3) were very similar to those of large DODAC vesicles (17), a fact that suggests size transformation. The difference in the absorbance value at 25°C before and after the heating-cooling cycle at 7 h (Fig. 3) could a priori be explained as disaggregation of small aggregated vesicles or as aggregation of large fused vesicles. For disaggregation to be the case, it could be expected that during the hours following the heating-cooling cycle the absorbance should again increase. Since the absorbance value remained unchanged for, at least, 24 h after the cycle (see Results), the absorbance decrease upon heating and cooling can be explained by a temperature induced fusion of small aggregated vesicles resulting in large vesicles that could aggregate during the cooling process.

The Derjaguin-Landau-Verwey-Overbeek (DLVO) theory for colloid stability is based upon long-range interactions due to electrostatic and electrodynamic (van der Waals) forces (34). It has been shown, both for lipids and synthetic amphiphiles, that the DLVO could not account for the relative stabilities of small and large vesicles in the presence of salt (6, 11). The DLVO neglects important short-range interparticle interactions such as those due to water structure around the polar headgroup (35). As a consequence, in spite of the role played by electrostatic repulsion and van der Waals attraction for the establishment of short-range interactions, hydration repulsion can be the limiting barrier for the fusion process. Since the DODAC molecule has two methyl groups in the cationic polar head, one may reasonably suppose that the surrounding hydration water is less tightly bound than that around a phosphate head group. Therefore, the hydration repulsive force at close approach due to water structure is lower for DODAC than for DHP vesicles in agreement with the higher frequency of fusion observed for the former. As the DPPC molecule possesses both the quaternary ammonium and the phosphate groups, one could speculate that the surrounding hydration shell of phospholipid bilayers (36) is more structured in comparison with that of the same separate groups in our synthetic bilayers, an hypothesis that partially accounts for the experimentally established stability of phospholipid vesicles in the range of 0.01–0.2 M monovalent salts.

In addition to the hydration shell around each head group, other factors can be involved in the short-range repulsion between phospholipid bilayers, such as a polymer-type steric repulsion due to the thermal mobility of the head groups (37). Since the head groups of DODAC or DHP are less bulky than those of lecithin, the steric short-range repulsion should be smaller for DODAC or DHP sonicated vesicles, leading to a higher frequency of adhesion and fusion under comparable conditions.

Finally, we will try to compose an energetic picture which could qualitatively describe interactions between DODAC or DHP vesicles during their mutual approach. First, calculated Stern potential values for sonicated DODAC vesicles are smaller than those for sonicated DHP vesicles (11), a fact that allows us to assume an energy barrier of repulsion (E) for sonicated DODAC vesicles that is lower than the corresponding barrier for sonicated DHP vesicles. Second, since aggregation occurs preferentially for sonicated DHP vesicles and fusion for sonicated DODAC vesicles, the supposition of a deeper attractive energy minimum (M) for sonicated DHP vesicles is justif-

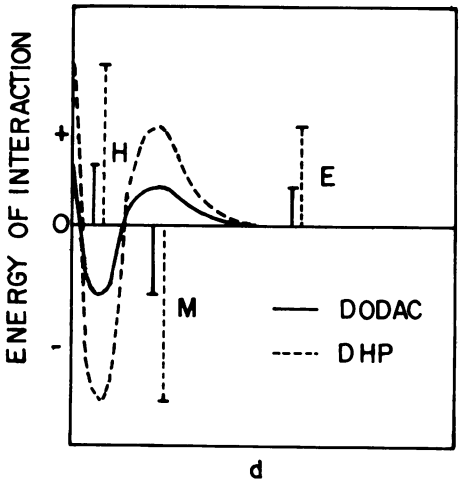

FIGURE 10 Hypothetical picture for the energy of interaction as a function of the separation distance (d) between sonicated DODAC or DHP vesicles. The positive sign refers to repulsive, and the negative, to attractive energies. The presence of energy barriers (E and H) and energy minimum (M) are justified in the text.

ied. Third, from simple structural considerations, the repulsive energy barrier (H) at zero separation distance due to hydration of the polar heads should be smaller for DODAC than for DHP. On these grounds, we propose the qualitative energy diagram in Fig. 10, which differentiates a configuration leading to fusion from another leading to aggregation.

We gratefully acknowledge Mr. Hélio Brandão and Dr. Antonio Sesso for the electron microscopy and Dr. Mari Armelin for careful revision of the manuscript. We thank also one of the referees for pertinent references and comments.

This work was supported by the Conselho Nacional de Desenvolvimento Cientifico e Technológico (CNPq) and Financiadora de Estudos e Projetos (FINEP).

Received for publication 20 December 1985 and in final form 9 April 1986.

REFERENCES

1. Gomperts, B. D. 1977. Models for membrane structure. *In* The Plasma Membrane: Models for Structure and Function. H. B. Jovanovich, editor. Academic Press, Inc., London. 1–49.
2. Fendler, J. H. 1980. Surfactant vesicles as membrane mimetic agents: characterization and utilization. *Acc. Chem. Res.* 13:7–13.
3. Chaimovich, H., J. B. S. Bonilha, D. Zanette, and I. M. Cuccovia. 1984. Analysis of the effect of micelles and vesicles on the reactivity of nucleophiles derived from the dissociation of weak acids. *In* Surfactants in Solution. K. L. Mittal and B. Lindman, editors. Plenum Publishing Corp., New York and London. 1121–1138.
4. Dimitrov, D. S., D. V. Zhflev, and R. K. Jain. 1985. Stability of membrane systems modeled as multilayered viscoelastic films. *J. Theor. Biol.* 113:353–377.
5. Nir, S., and J. Bentz. 1978. On the force between phospholipid bilayers. *J. Colloid Interface Sci.* 65:399–414.
6. Nir, S., J. Bentz, and N. Duezguenes. 1981. Two modes of reversible vesicle aggregation: particle size and the DLVO theory. *J. Colloid Interface Sci.* 84:266–269.
7. Bentz, J., and S. Nir. 1981. Mass action kinetics and equilibria of reversible aggregation. *J. Chem. Soc. Faraday Trans. I.* 77:1249–1275.
8. Ohki, S., N. Duezguenes, and K. Leonards. 1982. Phospholipid vesicle aggregation: effect of monovalent and divalent ions. *Biochemistry.* 21:2127–2133.
9. Rydhag, L., K. Rosenquist, P. Stenius, and L. Oedberg. 1983. Colloidal stability of liposomes. *In* Physical Chemistry of Surfactants in Solution. K. L. Mittal and E. J. Fendler, editors. Plenum Publishing Corp., New York.
10. Ohky, S., S. Roy, H. Ohshima, and K. Leonards. 1984. Monovalent cation-induced phospholipid vesicle aggregation: effect of ion binding. *Biochemistry.* 23:6126–6132.
11. Carmona-Ribeiro, A. M., L. S. Yoshida, and H. Chaimovich. 1985. Salt effects on the stability of dioctadecyldimethylammonium chloride and sodium dihexadecylphosphate vesicles. *J. Phys. Chem.* 89:2928–2933.
12. Rupert, L. A. M., D. Hoekstra, and J. B. F. N. Engberts. 1985. Fusogenic behaviour of didodecyldimethylammonium bromide bilayer vesicles. *J. Am. Chem. Soc.* 107:2628–2631.
13. Schales, O., and S. S. Schales. 1941. A simple and accurate method for the determination of chloride in biological fluids. *J. Biol. Chem.* 140:879–884.
14. Houser, G., S. Fleischer, and A. Yamamoto. 1970. Two dimensional thin layer chromatography separation of polar liquids and determination of phospholipids by phosphorus analysis of spots. *Lipids.* 5:494–496.
15. Tran, C. D., P. L. Klahn, A. Romero, and J. H. Fendler. 1978. Characterization of surfactant vesicles as potential membrane models. Effect of electrolytes, substrates and fluorescent probes. *J. Am. Chem. Soc.* 100:1622–1624.
16. Mortara, R. A., F. H. Quina, and H. Chaimovich. 1978. Formation of closed bilayers from a single phosphate diester. Preparation and some properties of vesicles of dihexadecyl phosphate. *Biochem. Biophys. Res. Commun.* 81:1080–1086.
17. Carmona-Ribeiro, A. M., and H. Chaimovich. 1983. Preparation and characterization of large dioctadecyldimethylammonium chloride liposomes and comparison with small sonicated vesicles. *Biochim. Biophys. Acta.* 733:172–179.
18. Carmona-Ribeiro, A. M., L. S. Yoshida, A. Sesso, and H. Chaimovich. 1984. Permeabilities and stability of large dihexadecylphosphate and dioctadecyldimethylammonium chloride vesicles. *J. Colloid Interface Sci.* 100:433–443.
19. Schenkman, S., P. S. Araujo, R. Dijkman, F. H. Quina, and H. Chaimovich. 1981. Effects of temperature and lipid composition on the serum albumin-induced aggregation and fusion of small unilamellar vesicles. *Biochim. Biophys. Acta.* 649:633–641.
20. Morgan, C. G., H. Williamson, S. Fuller, and C. Hudson. 1983. Melittin induces fusion of unilamellar phospholipid vesicles. *Biochim. Biophys. Acta.* 732:668–674.
21. Wilschut, J., and D. Papahadjopoulos. 1979. Ca^{2+}-induced fusion of phospholipid vesicles monitored by mixing of aqueous contents. *Nature (Lond.).* 281:690–692.
22. Herrmann, U., and J. H. Fendler. 1979. Low angle laser light scattering and photon correlation spectroscopy in surfactant vesicles. *Chem. Phys. Lett.* 64:270–274.
23. Yoshikawa, W., H. Akutsu, and Y. Kyogoku. 1983. Light-scattering properties of osmotically active liposomes. *Biochim. Biophys. Acta.* 735:397–406.
24. Chong, C. S., and K. Colbow. 1976. Light scattering and turbidity measurements on lipid vesicles. *Biochim. Biophys. Acta.* 436:260–282.
25. Koch, A. 1961. Some calculations on the turbidity of mitochondria and bacteria. *Biochim. Biophys. Acta.* 51:429–441.
26. Schmidt, C. F., D. Lichtenberg, and T. E. Thompson. 1981. Vesicle-vesicle interactions in sonicated dispersions of dipalmitoylphosphatidylcholine. *Biochemistry.* 20:4792–4797.
27. Lord Rayleigh. 1918. On the scattering of light by shells. *Proc. R. Soc. Lond. A. Math. Phys. Sci.* 94:296–300.
28. Mie, G. 1908. Beitrage zur optik trueber Medien steziell colloidaler Metaloesungen. *Ann. Physik.* 25:377–445.
29. Joebst, G. 1925. Strahlung dielektrischer Kugel in Grenzsalle das Kugelmaterial und umgebendes Medium fast gleich Brechungsgfindiceshaben. *Ann. Physik.* 78:157–166.
30. Johnson, S. M., and N. Buttress. 1973. The osmotic insensitivity of sonicated liposomes and the density of phospholipid-cholesterol mixtures. *Biochim. Biophys. Acta.* 307:20–26.
31. Reeves, J. P., and R. M. Dowben. 1970. Water permeability of phospholipid vesicles. *J. Membr. Biol.* 3:123–141.
32. Bangham, A. D., J. de Gier, and G. D. Greville. 1967. Osmotic properties and water permeability of phospholipid liquid crystals. *Chem. Phys. Lipids.* 1:225–246.
33. Wong, M., and T. E. Thompson. 1982. Aggregation of dipalmitoylphosphatidylcholine vesicles. *Biochemistry.* 21:4133–4139.
34. Verwey, E. J., and J. T. G. Overbeek. 1948. Theory of the Stability of Lyophobic Colloids. Elsevier, New York.
35. Ninham, B. 1981. Surface forces: the last 30 Å. *Pure Appl. Chem.* 53:2135–2147.
36. Le Neveu, D. M., R. P. Rand, V. A. Parsegian, and D. Gingell. 1977. Measurement and modification of forces between lecithin bilayers. *Biophys. J.* 18:209–230.
37. Marra, J., and J. Israelachvili. 1985. Direct measurements of forces between phosphatidylcholine and phosphatidylethanolamine bilayers in aqueous electrolyte solutions. *Biochemistry.* 24:4608–4618.